Developmental Biology 345 (2010) 237–245

Contents lists available at ScienceDirect

Developmental Biology

journal homepage: www.elsevier.com/developmentalbiology

Regional neural tube closure defined by the *Grainy head*-like transcription factors

Yeliz Rifat [a,1], Vishwas Parekh [b,1], Tomasz Wilanowski [a,2], Nikki R. Hislop [a], Alana Auden [a], Stephen B. Ting [a,3], John M. Cunningham [b], Stephen M. Jane [a,c,*]

[a] Bone Marrow Research Laboratories, Melbourne Health Research Directorate, c/o Royal Melbourne Hospital Post Office, Parkville, VIC 3050, Australia
[b] Department of Pediatrics, and The Committee on Developmental Biology, University of Chicago, Chicago, IL 60637, USA
[c] Department of Medicine, University of Melbourne, Parkville, VIC 3050, Australia

ARTICLE INFO

Article history:
Received for publication 12 June 2010
Accepted 14 July 2010
Available online 21 July 2010

Keywords:
Neural tube closure
Grainy head-like
Spina bifida
Exencephaly
Knock-out
Knock-in

ABSTRACT

Primary neurulation in mammals has been defined by distinct anatomical closure sites, at the hindbrain/cervical spine (closure 1), forebrain/midbrain boundary (closure 2), and rostral end of the forebrain (closure 3). Zones of neurulation have also been characterized by morphologic differences in neural fold elevation, with non-neural ectoderm-induced formation of paired dorso-lateral hinge points (DLHP) essential for neural tube closure in the cranial and lower spinal cord regions, and notochord-induced bending at the median hinge point (MHP) sufficient for closure in the upper spinal region. Here we identify a unifying molecular basis for these observations based on the function of the non-neural ectoderm-specific *Grainy head*-like genes in mice. Using a gene-targeting approach we show that deletion of *Grhl2* results in failed closure 3, with mutants exhibiting a split-face malformation and exencephaly, associated with failure of neuro-epithelial folding at the DLHP. Loss of *Grhl3* alone defines a distinct lower spinal closure defect, also with defective DLHP formation. The two genes contribute equally to closure 2, where only *Grhl* gene dosage is limiting. Combined deletion of *Grhl2* and *Grhl3* induces severe rostral and caudal neural tube defects, but DLHP-independent closure 1 proceeds normally in the upper spinal region. These findings provide a molecular basis for non-neural ectoderm mediated formation of the DLHP that is critical for complete neuraxis closure.

Introduction

Neurulation is the embryonic process in which the neural plate is formed and remodelled into the neural tube, the precursor of the brain and spinal cord. Neural tube defects (NTDs) reflect failures in this process and manifest in their most severe forms as exencephaly, spina bifida (SB), and craniorachischisis (Detrait et al., 2005; Harris and Juriloff, 2007). Historically, neural tube closure has been described at a cellular and anatomical level, largely because the molecular cues governing the process in the different regions of the developing nervous system have not been defined (Colas and Schoenwolf, 2001; Juriloff and Harris, 2000). Studies in mice have identified three closure points involved in primary neurulation (Golden and Chernoff, 1993; Sakai, 1989), and failure of each closure results in a distinct phenotype. Craniorachischisis is observed with failed closure 1, whereas embryos in which closure 2 fails exhibit exencephaly involving the midbrain/hindbrain regions. Failure of closure 3 leads to exencephaly involving the forebrain and extending to the mid/hindbrain, in association with a split-face malformation (Copp et al., 2003). Zones of neurulation have also been defined by differences in neural fold elevation (Juriloff and Harris, 2000). Bending of the neural plate occurs at two principal sites: the median hinge point (MHP) that overlies the notochord, and the paired dorso-lateral hinge points (DLHP) that are situated at the point of attachment of the surface ectoderm to the outside of each neural fold (Lawson et al., 2001; Shum and Copp, 1996). The MHP is induced by signals from the notochord, and is the sole site of bending in the upper spinal cord (Ybot-Gonzalez et al., 2002). In contrast, in the cranial and lower spinal cord regions, formation of the DLHP is essential for neural tube closure (Copp et al., 2003).

Although more than 100 mutant mouse genes disrupt neurulation, many of them display multiple developmental anomalies in addition to their NTDs, and few have provided broader insight into the regional signals for neural tube closure (Harris and Juriloff, 2007). Clear exceptions to this are the mutants of the planar cell polarity (PCP) signalling pathway, which exhibit a failure in closure 1, with resultant craniorachischisis (Curtin et al., 2003; Hamblet et al., 2002; Kibar et al., 2001; Montcouquiol et al., 2003; Murdoch et al., 2001; Murdoch et al., 2003; Wang et al., 2006). We now report that the members of the

* Corresponding author. Bone Marrow Research Laboratories, Melbourne Health Research Directorate, c/o Royal Melbourne Hospital Post Office, Parkville, VIC 3050, Australia. Fax: +61 3 93428634.
E-mail address: jane@wehi.edu.au (S.M. Jane).
[1] These authors contributed equally to this work.
[2] Current address: Laboratory of Signal Transduction, Nencki Institute of Experimental Biology, Polish Academy of Sciences, Warsaw, Poland.
[3] Current address: Cell Cycle and Cancer Genetics Laboratory, Peter MacCallum Cancer Centre, Melbourne, Australia.

0012-1606/$ – see front matter © 2010 Elsevier Inc. All rights reserved.
doi:10.1016/j.ydbio.2010.07.017

Grainy head-like (*Grhl*) family of developmental transcription factors provide distinct regional signals for rostral and caudal neural tube closure. We have previously demonstrated that mice lacking *Grhl3* exhibit fully penetrant thoraco-lumbo-sacral SB (Ting et al., 2003a). Exencephaly involving the midbrain was also observed in 3% of *Grhl3*-null embryos. Using additional gene knock-out and knock-in strategies, we now show that *Grhl2* and *Grhl3* play both unique and cooperative roles in establishing distinct zones of primary neurulation.

Materials and methods

Generation of Grhl2 heterozygous mice

The mouse *Grhl2* locus was isolated from a 129/SV/J genomic library with a cDNA fragment derived from the 5′ end of the gene. We cloned a 2.7 kb NotI–BamHI PCR-derived fragment into pβgalpAloxneo (Ting et al., 2003a), fusing the eleventh codon of *Grhl2* exon 2 to the ATG of β-galactosidase. The 3′ flanking region was a SalI–KpnI PCR-derived fragment extending 4.0 kb from the beginning of intron 3. The targeting vector was linearized with NotI and electroporated into W9.5 embryonic stem cells. G418-resistant clones, in which the targeting vector had recombined with the endogenous *Grhl2* gene were identified using HindIII-digested genomic DNA with the 3′ probe. This probe distinguished between the endogenous (6.1 kb) and targeted (7.5 kb) alleles. Two ES cell clones were used to generate mouse lines on a C57BL/6 background, and *Grhl2* heterozygous mice were identified by using Southern blotting as detailed above. Heterozygous mice were bred with *Cre*-deleter transgenic mice (Schwenk et al., 1995) to excise the *neo*^{r} cassette.

Genotyping of Grhl2 targeted mice

Mice were genotyped by PCR using genomic DNA prepared from tail biopsies or embryonic tissues. We generated the products of 363 bp from the wild type and 237 bp from the targeted *Grhl2* alleles. Primers used were specific for intron 1, common to the wild type and targeted *Grhl2* alleles (sense, 5′-TGAAGGTGTGAGTTGAGGCTTT-3′); exon 2, deleted from the targeted *Grhl2* allele (antisense, 5′-GTAGTAGTCATAGAGCAGGC-3′); and the *lacZ* cassette present only in the targeted *Grhl2* allele (antisense, 5′-CCCAGTCACGACGTTGTAAA-3′). PCR conditions were 94 °C for 2 min followed by 35 cycles of 94 °C for 30 s, 60 °C for 30 s and 72 °C for 1 min with a final 5 min extension at 72 °C.

Generation of Grhl3^{2ki} mice

An 1808 bp BamHI PCR-derived fragment containing the *Grhl2* cDNA was cloned into pβgalpAloxneo, fusing the twelfth codon of *Grhl3* exon 2 to the corresponding codon of *Grhl2*. The 3′ flanking region was a Sal1–Kpn1 fragment extending 2.6 kb from the beginning of intron 3. The vector was linearized with NotI and electroporated into W9.5 embryonic stem cells. G418-resistant clones in which the targeting vector had recombined with the endogenous *Grhl3* gene were identified using BamHI-digested genomic DNA probed with 5′ probe (data not shown). *Grhl3^{2ki}* mice were identified by hybridising BamHI-digested genomic DNA with the 3′ probe, which distinguished between endogenous (5.2 kb) and targeted (7.5 kb) alleles. Heterozygous mice were bred with *Cre*-deleter transgenic mice (Schwenk et al., 1995) to excise the *neo*^{r} cassette.

Genotyping of Grhl3^{2ki} mice

Mice were genotyped by PCR using genomic DNA prepared from tail biopsies or embryonic tissues. We generated products of 810 bp from the wild type and 539 bp from the targeted *Grhl3* allele. Primers used were specific for intron 1, common to the wild type and targeted *Grhl3* alleles (sense, 5′-GGATCAGAAGACCATGCC-3′); intron 2, deleted from the targeted *Grhl3* allele (antisense, 5′-AGGCTGTTA-GAGTTGGTG-3′); and the *Grhl3*/*Grhl2* cDNA fusion, present only in the targeted *Grhl3* allele (antisense, 5′-AGAGCTCTCGGTGATGGATA-3′). PCR conditions were 94 °C for 2 min followed by 35 cycles of 94 °C for 30 s, 60 °C for 30 s and 72 °C for 1 min with a final 5 min extension at 72 °C.

All animal experiments were pre-approved by the University of Melbourne and University of Chicago Animal Ethics Committees.

RT-PCR and Q-RT-PCR primer sequences and conditions

HPRT sense, 5′-GCTGGTGAAAAGGACCTCT-3′
HPRT antisense, 5′-CACAGGACTAGAACACCTGC-3′
Grhl3 sense, 5′-ACCGCTGTCAGCAAAATCTC-3′
Grhl3 antisense, 5′-CAGTATCCGCTTCTCCTTGG-3′
Grhl3^{2ki} sense, 5′-ACCGCTGTCAGCAAAATCTC-3′
Grhl3^{2ki} antisense, 5′-TGGCTGTCACTTGCTTTGCT-3′
Grhl2 sense, 5′-ACCCATCCACAGAGCATAC-3′
Grhl2 antisense, 5′-GCCTGAACATCCGCTTAAC-3′
β-actin sense, 5′-CGTTGACATCCGTAAAGACCTCTA-3′
β-actin antisense, 5′-TAAAACGCAGCTCAGTAACAGTCCG-3′
Grhl3 Q-RT-PCR sense, 5′-GCAAGCGAGGCATCCTGGTTAA-3′
Grhl3 Q-RT-PCR antisense, 5′-ACGTGGTTGCTGTAGTGTTGG-3′.

RT-PCR conditions for *HPRT*, *Grhl3* and *Grhl3^{2ki}* were 94 °C for 2 min followed by various cycles of 94 °C for 30 s, 60 °C for 30 s and 72 °C for 1 min, with a final extension period of 72 °C for 5 min. The annealing temperature used for *HPRT*-specific primers was 64 °C. The three primer pairs gave predicted size bands of 229 bp for *HPRT*, 388 bp for *Grhl3* and 336 bp for *Grhl3^{2ki}*. RT-PCR conditions for *Grhl2* and *β-actin* were 94 °C for 3 min followed by 32 cycles of 94 °C for 30 s, 56 °C for 30 s and 72 °C for 1 min with a final 5 min extension at 72 °C.

Q-RT-PCR was performed in a Rotorgene 2000 (Corbett Research) in a final volume of 20 μl. Reaction mixtures comprised 1× reaction buffer plus 2.5 mM (HPRT) or 3 mM (Grhl3) $MgCl_2$, 0.05 mM dNTPs (Roche), 0.1 μM gene-specific primers, 1 U Taq (Fisher Biotech), a 1/10,000 dilution of SYBR Green I (Molecular Probes), and 2 μl of sample or standard. Cycling conditions were 94 °C for 15 s, 55 °C (Grhl3) or 52 °C (HPRT) for 30 s and 72 °C for 30 s.

Histology, in situ hybridisation, SEM, and whole mount skeletal staining

Embryos from *Grhl3^{2ki}* intercrosses were immersion fixed in 4% paraformaldehyde in phosphate buffered saline, pH 7.3 and embedded in paraffin. Sections were stained with hematoxylin and eosin. *In situ* hybridisation was performed as described previously (Auden et al., 2006). The RNA probes utilised were generated against unique portions of the genes, and were specific for individual family members. [^{33}P] UTP (Perkin-Elmer, MA) labelled antisense RNA probes of *Grhl3^{2ki}* (rabbit β-globin polyA tail, nt 12172–13366, in Bluescript II SK plasmid), *Grhl2* (nt 328–743 in PCR2.1-Topo), and *Grhl3* (nt 404–889 in pSPT19) were transcribed using T7 RNA polymerase (Roche, Germany). The probes did not cross react with other members of the *Grhl*-like family (data not shown). For SEM analysis, embryos were fixed overnight in 1% electron microscopy-grade gluteraldehyde, rinsed in 0.1 mol/L sodium cacodylate buffer with 5% sucrose, post-fixed in 1% OsO4 in the same buffer for 1 hour and stained with 4% uranyl acetate in water for 2 h. This was followed by dehydration in a graded series of ethanol to bring the embryos to absolute ethanol. Subsequently, the embryos were exposed to critical point drying in a Samdri 520 system (Tousimis, Rockville, MD) and viewed using an FEI Phillips XL30 Environmental Scanning Electron

Microscope. Whole mount skeletal staining on E17.5 embryos was performed as described previously (McLeod, 1980).

Results

Grhl2-null mice exhibit split-face and NTDs

To determine the functional role of *Grhl2* in mammalian neurulation, we generated a 4.2 kb deletion in the *Grhl2* genomic locus by gene-targeting, and confirmed that this resulted in a null allele (Figs. 1A–D). Intercrosses of $Grhl2^{+/-}$ mice produced no viable *Grhl2*-null pups, and timed pregnancies defined embryonic lethality of this genotype at approximately E11.5 (Supplementary Table 1). The null embryos exhibited a fully penetrant split-face malformation, associated with cranioschisis (Figs. 2A–C). Closure of the remainder of the neural tube occurred normally, with the exception of the posterior neuropore (PNP), which remained open in all embryos (Figs. 2B and C). To examine neural fold elevation, histological sections at the level of the PNP from $Grhl2^{-/-}$ embryos at the 15–25 somite stage were compared with wild type controls, and *Grhl3*-null mutants (Figs. 2D–F) (Ybot-Gonzalez et al., 2007a). Although the MHP developed normally in the $Grhl2^{-/-}$ embryos, the DLHP failed to form, and closure did not proceed beyond this point. This appearance was identical to that observed in the *Grhl3*-null embryos. Sections from the spinal cord above the neural tube defect in the $Grhl2^{-/-}$ embryos demonstrated that both MHP and DLHP formation occurred normally in this region (Fig. 2G). Additional histological analysis failed to determine the cause of the embryonic lethality in the *Grhl2*-null mice (data not shown).

Genetic interactions between Grhl2 and Grhl3 in rostral and caudal neural tube closure

To evaluate genetic interactions, and the effects of *Grhl* gene dosage on neural tube closure, we generated lines lacking two or more *Grhl2*/*Grhl3* alleles As newborn mice with NTDs are cannibalised by their mothers, we confined our analysis to embryos between E10.5 and E18.5, initially examining compound heterozygotes ($Grhl2^{+/-}$/$Grhl3^{+/-}$) at a range of developmental time points. Although mice heterozygous at either locus develop normally, loss of one allele of each gene resulted in NTDs of varying severity in 13% of embryos, indicative of a functional interaction between these genes (Fig. 3B and Table 1). Exencephaly in the compound heterozygotes (5%) involved only the mid- and hindbrain, characteristic of failed closure 2, and was analogous in appearance to the cranial NTDs observed in the $Grhl3^{-/-}$ embryos (Ting et al., 2003a). The incidence of exencephaly in the $Grhl2^{+/-}$/$Grhl3^{+/-}$ embryos was similar to that observed in the $Grhl3^{-/-}$ embryos, suggesting that the two genes play cooperative roles in mid–hindbrain closure, and that the dosage of the genes is the limiting factor for closure, rather than the function of a specific *Grhl* family member. At this stage we are unable to distinguish whether exencephaly results from a complete failure of closure 2, or alternatively, failed caudal extension from the initial closure point.

We next examined mice lacking the *Grhl3* gene, and heterozygous for the targeted *Grhl2* allele. $Grhl2^{+/-}$/$Grhl3^{-/-}$ embryos exhibited fully penetrant thoraco-lumbo-sacral SB, as is observed in embryos lacking *Grhl3* alone (Ting et al., 2003a). In addition, they also displayed fully penetrant exencephaly involving the mid- and hindbrain (Fig. 3C). Facial fusion and forebrain closure were normal in these embryos. These findings support our hypothesis that the two *Grhl* genes play equivalent roles in closure 2 (or its extension), and that gene dosage is the pivotal factor in determining whether this will occur. They also indicate that initiation of closure 3 occurs independently of *Grhl3*, even in the context of reduced dosage of *Grhl2*. We extended our analysis of the genetic interaction of the *Grhl* factors by examining embryos by scanning electron microscopy (SEM) with the genotype $Grhl2^{-/-}$/$Grhl3^{+/-}$ at E10.5, due to the early lethality of the *Grhl2*-null mice. These embryos displayed failed cranio-facial fusion and cranioschisis. Unexpectedly, they also displayed fully penetrant thoraco-lumbo-sacral SB that extended rostrally to the identical level observed in the *Grhl3*-null embryos (Fig. 3F). Closure of a small region of the neural tube between the mid-thoracic region and the hindbrain/cervical cord boundary, the site of

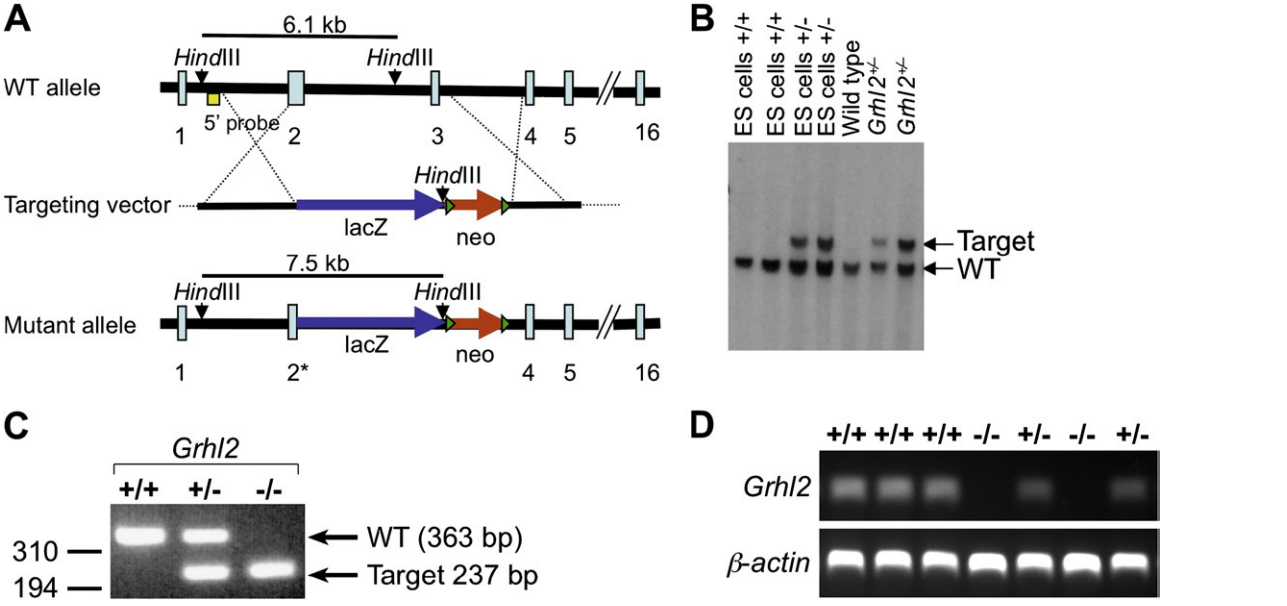

Fig. 1. Generation of $Grhl2^{-/-}$ embryos. (A) Gene-targeting strategy applied to the mouse *Grhl2* locus. The 5′ probe used for Southern analysis of the targeted allele is shown. (B) Southern analysis of the parental ES cell lines (+/+), two targeted ES cell clones (+/−), and wild type and heterozygous ($Grhl2^{+/-}$) mice with the 5′ flanking probe. (C) PCR genotyping of embryos. WT, product of wild type *Grhl2* allele; target, product of targeted *Grhl2* allele. (D) RT-PCR analysis of *Grhl2* and *β-actin* mRNA expression in E9.5 embryos (genotypes as indicated).

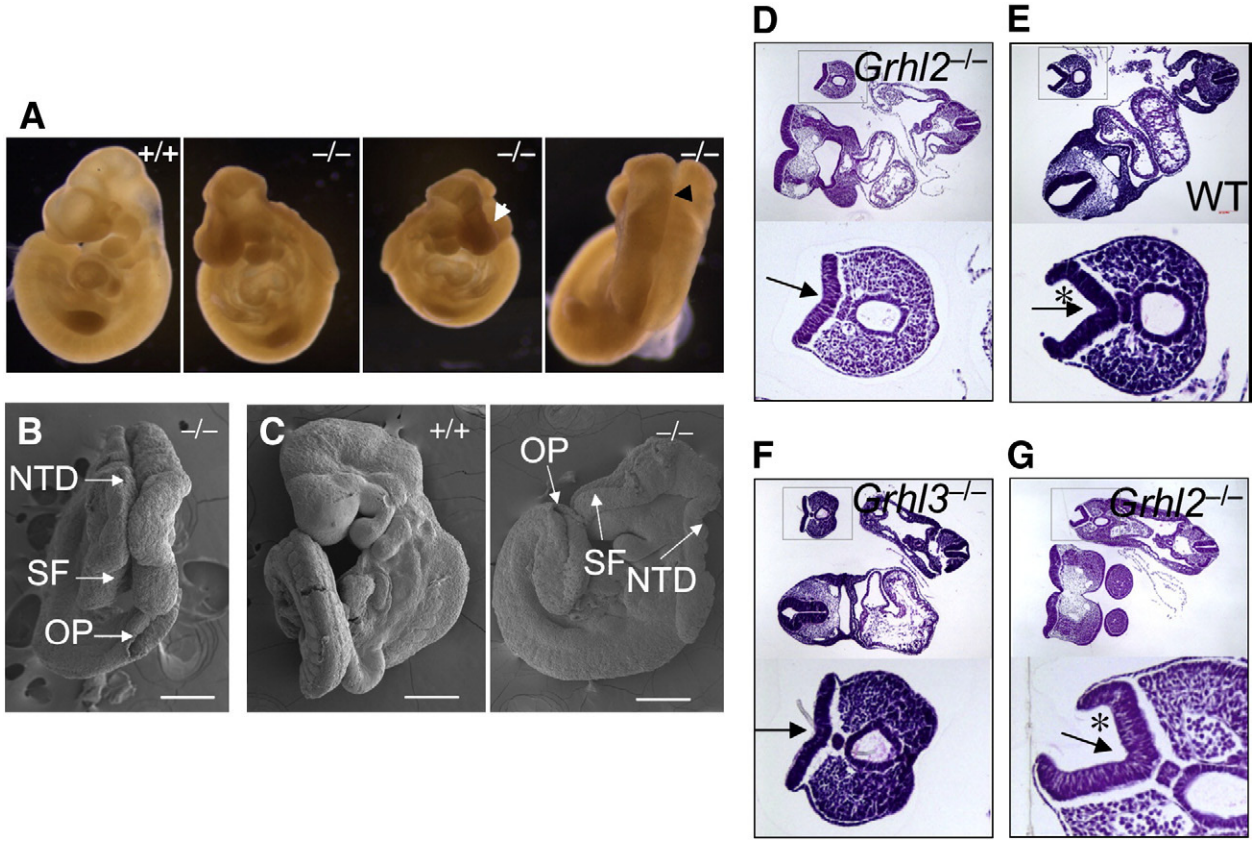

Fig. 2. *Grhl2* is essential for cranio-facial fusion and cranial neural tube closure. (A) Failure of cranial neural tube closure and fronto-nasal fusion in *Grhl2*-null (−/−) embryos compared with a wild type littermate (+/+) at E9.5 gestation. All null embryos had identical phenotypes (N = 85). Only animals containing identical numbers of somites were compared. The white arrow indicates the split-face abnormality, and the black arrow indicates the cranial NTD. (B) SEM of *Grhl2*-null embryo at E10.5 (superior view) demonstrating the NTD, split-face (SF), and open PNP (OP) abnormalities. (C) SEM of *Grhl2*-null embryo and wild type littermate at E10.5 (lateral view) demonstrating the NTD, split-face (white arrow) and open PNP (black arrow) abnormalities in the mutant. (D–F) Transverse H&E stained sections through $Grhl2^{-/-}$, $Grhl3^{-/-}$, and wild type (WT) embryos at the 15–25 somite stage. The level of the PNP is expanded below. (G) Transverse H&E stained section through a $Grhl2^{-/-}$ embryo at the level of the spinal cord above the neural tube defect. Arrows represent the median hinge point; asterisks represent one of the dorso-lateral hinge points.

closure point 1, proceeded normally in these embryos. Finally, we examined the phenotype of the $Grhl2^{-/-}/Grhl3^{-/-}$ embryos at E10.5. We observed that these embryos were indistinguishable from the $Grhl2^{-/-}/Grhl3^{+/-}$ mice, retaining closure of only the cervico-upper thoracic cord (Figs. 3G and H). These findings indicate that closure of this region, which initiates at closure point 1, occurs independently of the *Grhl* genes.

Grhl2 and Grhl3 are not functionally equivalent in neural tube closure

The non-redundant functions of *Grhl2* and *Grhl3* in rostral and caudal neural tube closure were observed despite the two genes exhibiting substantial sequence homology (Ting et al., 2003b), and displaying overlapping expression patterns at the time of neural tube closure (Auden et al., 2006). This dichotomy was emphasized further by our demonstration that the DNA consensus-binding site of GRHL2 was identical to the site previously defined for GRHL3 (Ting et al., 2005) (Supplementary Fig. 1). We therefore designed a knock-in model, in which *Grhl2* expression was regulated by the *Grhl3* genomic locus, as a stringent genetic test to further explore the functional equivalence of the two genes in neural tube closure (Figs. 4A–C). Mice heterozygous and homozygous for the knock-in ($Grhl3^{2ki}$) allele were generated. RT-PCR analysis using primers specific for the *Grhl3* and $Grhl3^{2ki}$ transcripts demonstrated that the knock-in allele was expressed in both the +/*2ki* and *2ki*/*2ki* animals, but not in the wild type controls. In contrast, endogenous *Grhl3* expression was observed in the wild type and *ki*/+ heterozygous mice, but not in the *2ki*/*2ki* homozygous mice (Fig. 4D). *In situ* hybridisation studies with *Grhl3* and $Grhl3^{2ki}$-specific probes demonstrated that the spatio-temporal expression pattern of the knock-in allele mirrored that of endogenous *Grhl3* during neural tube closure (Fig. 4E), and later in development in the epidermis (Supplementary Fig. 2).

$Grhl3^{+/2ki}$ animals were inter-crossed to yield homozygous knock-in embryos ($Grhl3^{2ki/2ki}$), or bred with $Grhl3^{+/-}$ mice to generate $Grhl3^{-/2ki}$ embryos. *Grhl3* expression was undetectable by RT-PCR in embryos with both these genotypes (Fig. 4D, and data not shown). Although the $Grhl3^{2ki/2ki}$ and $Grhl3^{-/2ki}$ mice were not represented at weaning, both genotypes were observed in normal Mendelian ratios at E18.5. Of the fifty-four $Grhl3^{2ki/2ki}$ (N = 32), and $Grhl3^{-/2ki}$ (N = 22) embryos examined, 96% exhibited SB confined to the lumbo-sacral region of the spinal cord (Fig. 5A, upper panel). In one embryo of each genotype, the NTD extended rostrally to involve the low thoracic region, but the mid-thoraco-lumbo-sacral SB observed in all *Grhl3*-null embryos (Fig. 5A, lower panel) was never observed. Similarly, exencephaly was never observed in these embryos, confirming our hypothesis that the two genes act through an identical mechanism in initiation of closure 2. The difference in severity of SB between the $Grhl3^{-/2ki}$ and $Grhl3^{2ki/2ki}$ embryos compared with the $Grhl3^{-/-}$ embryos was evident in skeletal preparations, which demonstrated splayed vertebrae at T11 in the most severely affected $Grhl3^{-/2ki}$ and $Grhl3^{2ki/2ki}$ embryos, compared to the level of T7 in the $Grhl3^{-/-}$ mice (Fig. 5B). There was no

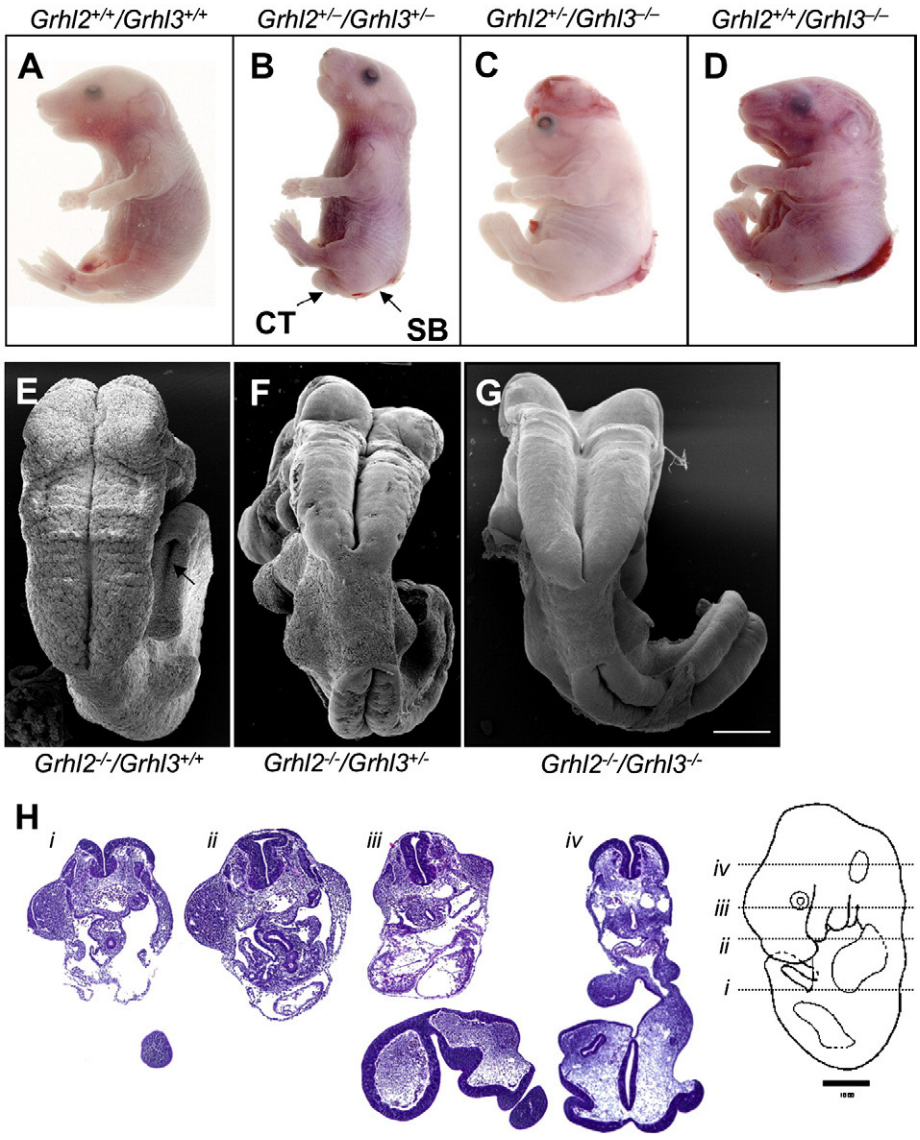

Fig. 3. Unique and cooperative roles of the *Grhl* genes in neural tube closure. (A) Wild type embryo. (B) Sacral SB and curled tail (CT) in a $Grhl2^{+/-}/Grhl3^{+/-}$ embryo. (C) Exencephaly and thoraco-lumbo-sacral SB in a $Grhl2^{+/-}/Grhl3^{-/-}$ embryo. (D) A $Grhl3^{-/-}$ embryo is shown for comparison. (E) NTD in $Grhl2^{-/-}$ embryos. The arrow demonstrates the open PNP. (F, G) Rostral and caudal NTDs in $Grhl2^{-/-}/Grhl3^{+/-}$ and $Grhl2^{-/-}/Grhl3^{-/-}$ embryos, with preservation of closure 1. (H) Transverse sections through a $Grhl2^{-/-}/Grhl3^{-/-}$ embryo at the levels indicated in the schematic.

difference in severity of the SB between $Grhl3^{2ki/2ki}$ and $Grhl3^{-/2ki}$ embryos, indicating that a single $Grhl3^{2ki}$ allele was capable of rescuing closure of the thoracic spinal cord in the absence of *Grhl3*.

Expression of proposed mediators of DLHP formation are not altered in $Grhl3^{-/-}$ mice

Although the analysis of many mutant mouse strains has led to the identification of factors involved in dorso-lateral bending of the neural plate (Copp, 2005), to date, only two genes that are expressed at the epidermal/neuro-epithelial interface have been implicated in this process, *BMP2* (Ybot-Gonzalez et al., 2007a) and *Noggin* (Stottmann et al., 2006). $BMP2^{-/-}$ mice, which die between E7.0 and E10.5, display multiple developmental perturbations, including severe growth retardation, an open proamniotic canal and abnormal cardiac development (Zhang and Bradley, 1996). Zhang and Bradley (1996) reported that they also displayed an open neural tube, whereas Ybot-Gonzalez et al. describe premature formation of the DLHP in the PNP in the mice at E9.5 (Ybot-Gonzalez et al., 2007a). $Noggin^{-/-}$ embryos display incompletely penetrant exencephaly (McMahon et al., 1998; Stottmann et al., 2006) associated with a loss of DLHP formation. Although the embryos also display lumbar SB in late gestation, the neural tube initially closes normally in this region, only to re-open with the formation of bloody cysts (Stottmann et al., 2006). To explore the mechanism underpinning the failure of DLHP formation in the *Grhl3*-null embryos, we compared the expression of *BMP2* and *Noggin* in the region of the PNP in these mice and wild type littermate controls at E8.5, immediately prior to DLHP formation. We also examined the expression of *Zic2*, which is expressed in the neuro-

Table 1
Neural tube defects of the $Grhl2^{+/-}/Grhl3^{+/-}$ embryos.

Genotype	Number of embryos[a]	Phenotype
$Grhl2^{+/-}/Grhl3^{+/-}$	83	Normal
	3	Exencephaly alone
	2	Exencephaly and curled tail
	2	Curled tail alone
	6	Low sacral SB and curled tail
Total	96	

[a] Embryos were harvested between E9.5 and E18.5.

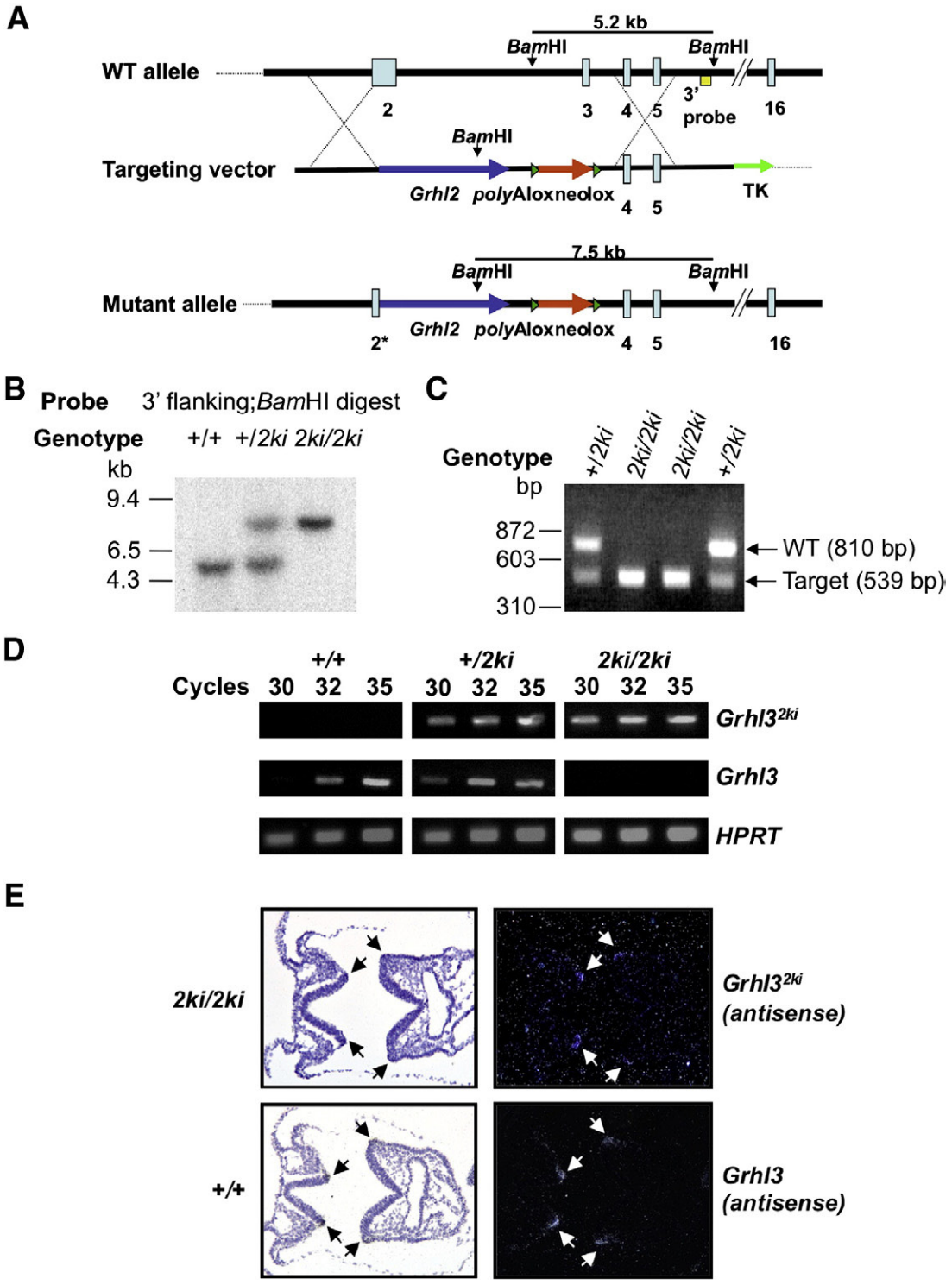

Fig. 4. Generation of mice carrying a *Grhl3*^{2ki} allele. (A) Gene-targeting strategy applied to generate the *Grhl3*^{2ki} allele. The 3′ probe used for Southern analysis of the targeted allele is shown. (B) Southern analysis of wild type (+/+), heterozygous (+/*2ki*) and homozygous (*2ki*/*2ki*) mice with the 3′ flanking probe. (C) PCR genotyping of embryos. WT, product of wild type *Grhl3* allele; target, product of targeted *Grhl3*^{2ki} allele. (D) RT-PCR analysis of *Grhl3*^{2ki}, *Grhl3*, and *HPRT* mRNA expression in E18.5 embryo epidermis (genotypes and PCR cycle numbers as indicated). (E) Transverse section of E8.5 *Grhl3*$^{2ki/2ki}$ (*2ki*/*2ki*) and wild type (+/+) embryos analysed by *in situ* hybridisation with antisense riboprobes specific for the *Grhl3*^{2ki} and *Grhl3* transcripts respectively. Arrows show expression in the non-neural ectoderm immediately adjacent to the folding neural plate in both embryos.

epithelium, but has been implicated in DLHP formation (Ybot-Gonzalez et al., 2007a). As shown in Fig. 6, the expression of all three genes was unchanged in the mutants, indicating that the key *Grhl* targets in DLHP formation are genes that have not previously been linked to this process.

Discussion

Although multiple genes have been implicated in neurulation in mice, our studies identify a single gene family that functionally demarcates distinct regions of neural tube closure (Fig. 7). In the

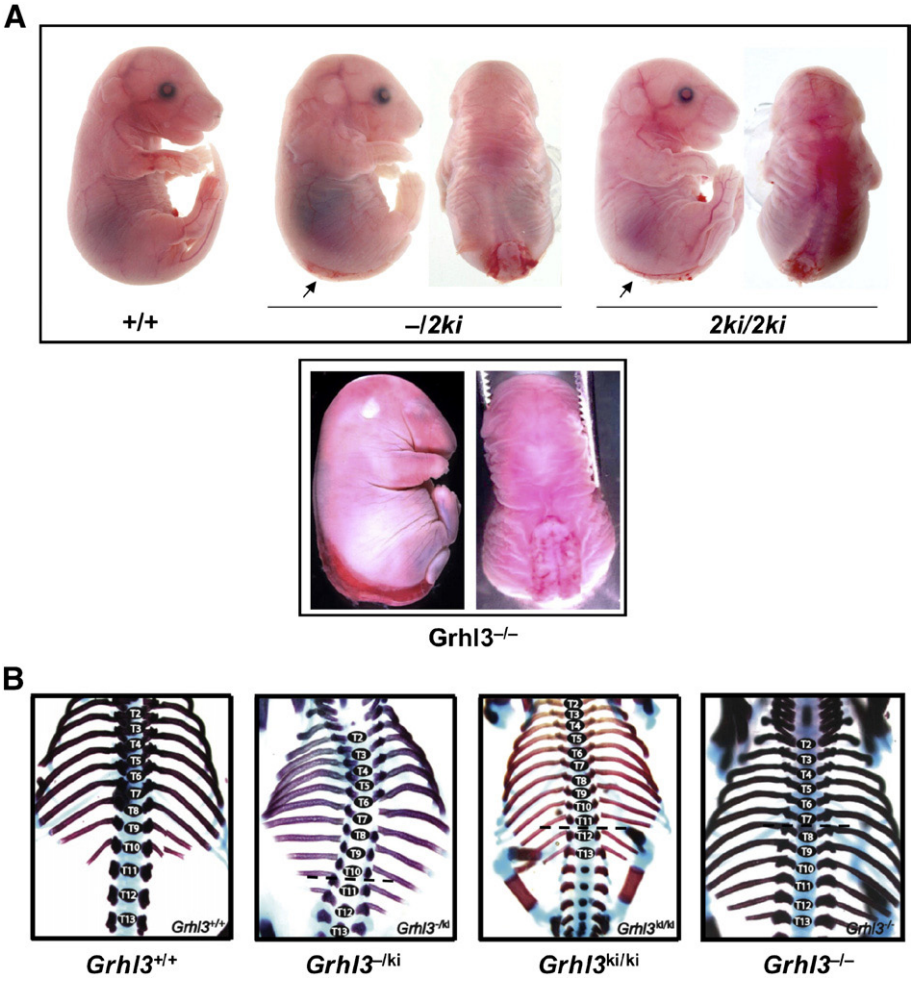

Fig. 5. *Grhl2* and *Grhl3* are not functionally equivalent in neural tube closure. (A) NTDs of varying severity in *Grhl3*$^{-/2ki}$ (−/2*ki*) and *Grhl3*$^{2ki/2ki}$ (2*ki*/2*ki*) embryos with a wild type (+/+) littermate control. A *Grhl3*$^{-/-}$ embryo is shown for comparison. The arrows indicate the NTDs. (B) Alizarin red/Alcian blue stained skeletal preparations of the thoracic spine in E18.5 embryos with the indicated genotypes illustrating abnormally splayed vertebral pedicles below the red arrows in the mutants.

cranial region, *Grhl2* is essential for closure 3, and analogous to other mutants that affect this closure (*Hes-1*, *Ski*, *AP-2*, and retinoic acid receptors) (Berk et al., 1997; Ishibashi et al., 1995; Lohnes et al., 1994; Schorle et al., 1996; Zhang et al., 1996), *Grhl2*-null embryos also exhibit failed closure 2. *Grhl2* and *Grhl3* function cooperatively in closure 2 (or its extension), and only gene dosage is critical for the prevention of mid–hindbrain exencephaly. Closure 1 occurs independently of *Grhl* gene function, and appears to be solely regulated by genes of the PCP pathway (Copp et al., 2003; Ybot-Gonzalez et al., 2007b). In the caudal regions, *Grhl3* functionally defines a novel spinal closure region, being essential for the prevention of SB below the mid-thoracic region. Finally, the two genes contribute equally to closure of the PNP, but via independent mechanisms, as evidenced by their inability to compensate for loss of the other in the context of either endogenous or knock-in alleles.

The zones defined by the different *Grhl* signatures encompass many of the features detailed in previous classifications based on morphology of neural fold elevation, and anatomical closure points (Copp et al., 2003; Juriloff and Harris, 2000). Closure of the cranial region and lower spinal cord is dependent on formation of the DLHP, whereas the upper spinal region requires only MHP formation. Studies with cultured mouse embryos have shown that *sonic hedgehog* (*Shh*) that emanates from the notochord inhibits DLHP formation in the upper spinal levels, and that the strength of *Shh* signalling lessens as the wave of spinal neurulation passes down the neuraxis allowing DLHP formation (Ybot-Gonzalez et al., 2002). More recently, *BMP2* signalling from the surface ectoderm has been shown to inhibit DLHP formation, and conversely, the *Bmp* antagonist *Noggin* stimulates bending (Ybot-Gonzalez et al., 2007a). *Zic2* also plays a role in DLHP formation, but the expression of this gene and *BMP2* and *Noggin* were unaltered in *Grhl3*-null embryos during neurulation. Both the *Grhl2* and *Grhl3*-null embryos do not form DLHP in the regions of failed neural tube closure, suggesting that these genes play an active role in this process. Commensurate with this, the two genes are expressed in the non-neural ectoderm adjacent to the folding neural plate at the time of neurulation. Epidermal ectoderm is both necessary and sufficient to induce folding of the neural plate in tissue isolation experiments (Hackett et al., 1997; Moury and Schoenwolf, 1995). Our data indicates that, in addition to *Bmp2* signalling, GRHL2 and GRHL3 are key regulators of this program, although the target genes through which this effect is mediated remain elusive. Our observation that the only region of the neural tube that does not depend on *Grhl* gene function for closure is the upper spinal cord, in which DLHP formation is not required (Copp et al., 2003) supports the importance of these factors in this process.

In the cranial region, additional mechanisms integral to DLHP formation have been identified through analysis of mouse mutants (Copp, 2005). These include a balance between neuro-epithelial proliferation and cell death, contraction of apical actin microfilaments, and emigration of cranial neural crest (CNC) cells. This latter process begins well in advance of cranial neural tube closure, unlike in the spinal region where emigration does not occur until after neural tube

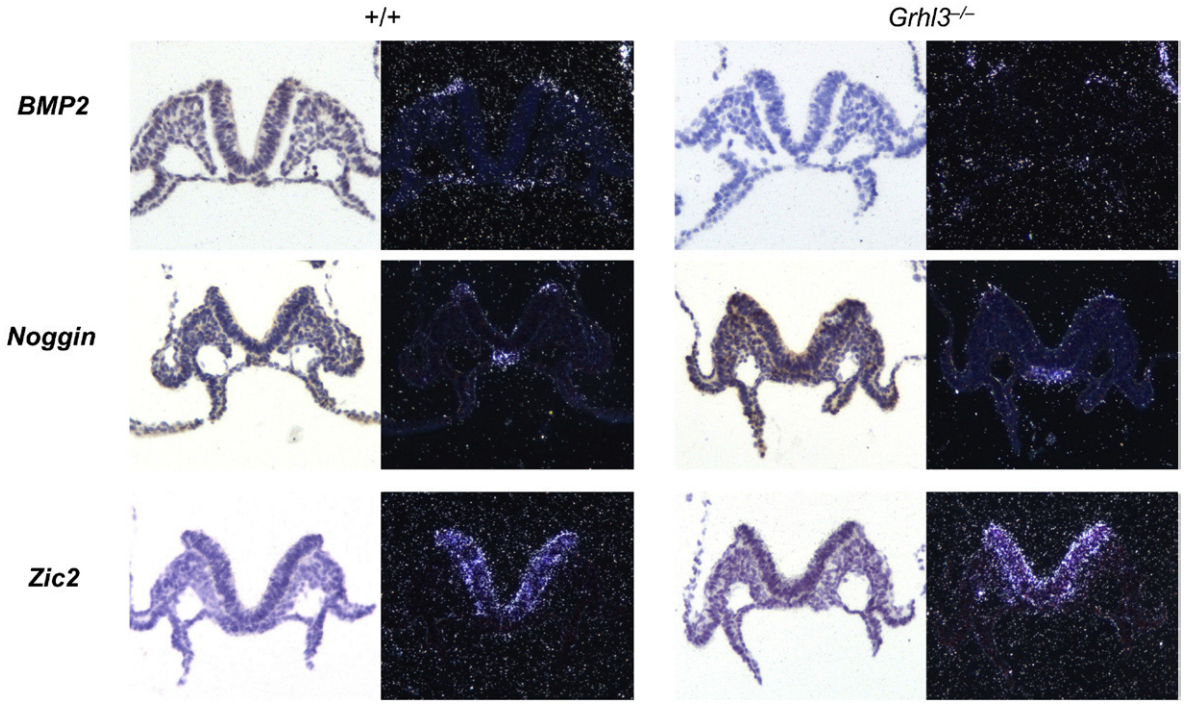

Fig. 6. The expression of genes linked to DLHP formation are not altered in *Grhl3*$^{-/-}$ mutants. Transverse section of E8.5 wild type (+/+) and *Grhl3*$^{-/-}$ embryos analysed by *in situ* hybridisation with antisense riboprobes specific for *BMP2*, *Noggin*, and *Zic2*.

closure is complete (Morriss-Kay and Tan, 1987). Our studies of the *Grhl2* gene in *Xenopus laevis* have defined a role for this factor in migration of cranial neural crest (CNC) cells (van Stry et al., submitted manuscript). Targeted deletion of other murine paralogues of anamniotic CNC regulatory genes manifest with defects in cranial neural tube closure, and cranio-facial development (Santagati and Rijli, 2003; Sauka-Spengler and Bronner-Fraser, 2006). Mice with mutations or knockouts of *Cited 2* (Bamforth et al., 2001) *Pax3* (Epstein et al., 1991), and *Twist* (Chen and Behringer, 1995) genes all exhibit CNC defects with mid–hindbrain exencephaly. In contrast, mice lacking the transcription factor AP-2 display a split-face malformation and cranioschisis, in addition to CNC defects (Schorle et al., 1996; Zhang et al., 1996). Our data with *Grhl2* suggests that it plays CNC-dependent and independent roles in cranial neural tube closure. In the *Grhl2*-null embryos, the observed phenotype mirrors the AP-2 knock-out mice, and is associated with CNC defects, including abnormal development of cranial ganglia (van Stry et al., submitted manuscript). However, the mid–hindbrain exencephaly observed in *Grhl2*/*Grhl3* compound heterozygotes, and *Grhl2*$^{+/-}$/*Grhl3*$^{-/-}$ embryos is not associated with CNC defects, suggesting that closure of this region occurs via a different mechanism. Interestingly, mid–hindbrain exencephaly, in the absence of CNC defects is also observed in AP-2 heterozygous mice suggesting that distinct mechanisms also govern the different regional closures induced by this factor (Kohlbecker et al., 2002).

The lack of effect of *Grhl2* and *Grhl3* expression on closure 1 underpins the importance of the PCP genes in mediating this event. Our data indicates that convergent extension is sufficient for closure in the cervico-thoracic region (Wallingford and Harland, 2002). However, beyond this domain, approximation of the neural folds

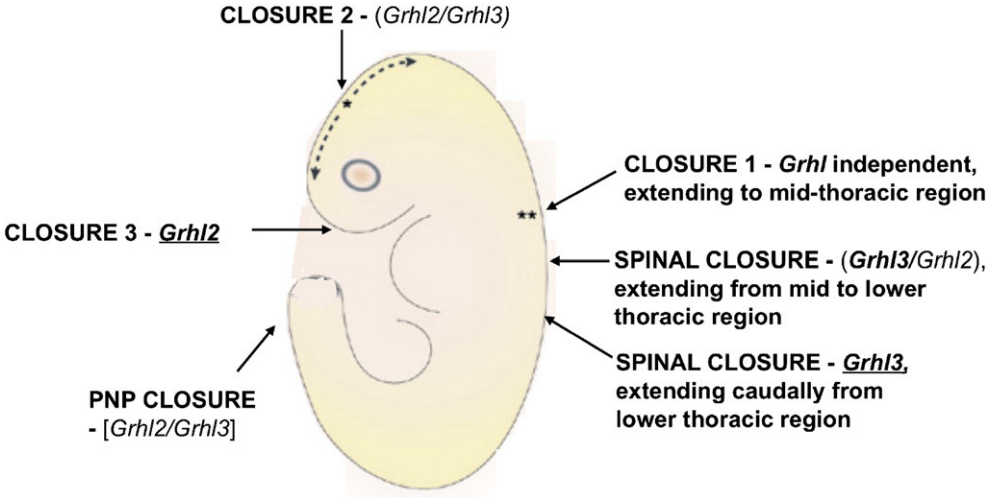

Fig. 7. Demarcation of the regions of neural tube closure based on the functions of the *Grhl* genes. Underline represents unique activity in that region. () represent cooperative activity in that region. [] represent overlapping, but non-cooperative action in that region. Bold represents dominant activity in that region.
Adapted from Copp et al. (2003).

alone is insufficient to allow closure to occur, and further bending of the neural plate at the DLHP induced by the *Grhl* factors is essential.

Acknowledgments

We thank Andrew Copp for his critical reading of the manuscript and helpful suggestions, members of the Jane lab for the discussion, and S. Hunjan and Ozgene Inc. (Perth, Australia) for the technical assistance. Animal support was provided by the staff from the Universities of Melbourne and Chicago, St. Jude Children's Research Hospital, and The Walter & Eliza Hall Institute. S.M.J. is a Principal Research Fellow of the Australian National Health and Medical Research Council (NHMRC). S.B.T. was supported by the Cancer Council of Australia. V.P. and J.M.C. were supported by the National Institutes of Health. The work was supported by Project Grants from the Australian NHMRC, and a Grant from the March of Dimes Foundation.

Appendix A. Supplementary data

Supplementary data associated with this article can be found, in the online version, at doi:10.1016/j.ydbio.2010.07.017.

References

Auden, A., Caddy, J., Wilanowski, T., Ting, S.B., Cunningham, J.M., Jane, S.M., 2006. Spatial and temporal expression of the Grainyhead-like transcription factor family during murine development. Gene Expr. Patterns 6, 964–970.

Bamforth, S.D., Braganca, J., Eloranta, J.J., Murdoch, J.N., Marques, F.I., Kranc, K.R., Farza, H., Henderson, D.J., Hurst, H.C., Bhattacharya, S., 2001. Cardiac malformations, adrenal agenesis, neural crest defects and exencephaly in mice lacking Cited2, a new Tfap2 co-activator. Nat. Genet. 29, 469–474.

Berk, M., Desai, S.Y., Heyman, H.C., Colmenares, C., 1997. Mice lacking the ski proto-oncogene have defects in neurulation, craniofacial, patterning, and skeletal muscle development. Genes Dev. 11, 2029–2039.

Chen, Z.F., Behringer, R.R., 1995. twist is required in head mesenchyme for cranial neural tube morphogenesis. Genes Dev. 9, 686–699.

Colas, J.F., Schoenwolf, G.C., 2001. Towards a cellular and molecular understanding of neurulation. Dev. Dyn. 221, 117–145.

Copp, A.J., 2005. Neurulation in the cranial region—normal and abnormal. J. Anat. 207, 623–635.

Copp, A.J., Greene, N.D., Murdoch, J.N., 2003. The genetic basis of mammalian neurulation. Nat. Rev. Genet. 4, 784–793.

Curtin, J.A., Quint, E., Tsipouri, V., Arkell, R.M., Cattanach, B., Copp, A.J., Henderson, D.J., Spurr, N., Stanier, P., Fisher, E.M., Nolan, P.M., Steel, K.P., Brown, S.D., Gray, I.C., Murdoch, J.N., 2003. Mutation of Celsr1 disrupts planar polarity of inner ear hair cells and causes severe neural tube defects in the mouse. Curr. Biol. 13, 1129–1133.

Detrait, E.R., George, T.M., Etchevers, H.C., Gilbert, J.R., Vekemans, M., Speer, M.C., 2005. Human neural tube defects: developmental biology, epidemiology, and genetics. Neurotoxicol. Teratol. 27, 515–524.

Epstein, D.J., Vekemans, M., Gros, P., 1991. Splotch (Sp2H), a mutation affecting development of the mouse neural tube, shows a deletion within the paired homeodomain of Pax-3. Cell 67, 767–774.

Golden, J.A., Chernoff, G.F., 1993. Intermittent pattern of neural tube closure in two strains of mice. Teratology 47, 73–80.

Hackett, D.A., Smith, J.L., Schoenwolf, G.C., 1997. Epidermal ectoderm is required for full elevation and for convergence during bending of the avian neural plate. Dev. Dyn. 210, 397–406.

Hamblet, N.S., Lijam, N., Ruiz-Lozano, P., Wang, J., Yang, Y., Luo, Z., Mei, L., Chien, K.R., Sussman, D.J., Wynshaw-Boris, A., 2002. Dishevelled 2 is essential for cardiac outflow tract development, somite segmentation and neural tube closure. Development 129, 5827–5838.

Harris, M.J., Juriloff, D.M., 2007. Mouse mutants with neural tube closure defects and their role in understanding human neural tube defects. Birth Defects Res. A Clin. Mol. Teratol. 79, 187–210.

Ishibashi, M., Ang, S.L., Shiota, K., Nakanishi, S., Kageyama, R., Guillemot, F., 1995. Targeted disruption of mammalian hairy and Enhancer of split homolog-1 (HES-1) leads to up-regulation of neural helix–loop–helix factors, premature neurogenesis, and severe neural tube defects. Genes Dev. 9, 3136–3148.

Juriloff, D.M., Harris, M.J., 2000. Mouse models for neural tube closure defects. Hum. Mol. Genet. 9, 993–1000.

Kibar, Z., Vogan, K.J., Groulx, N., Justice, M.J., Underhill, D.A., Gros, P., 2001. Ltap, a mammalian homolog of Drosophila Strabismus/Van Gogh, is altered in the mouse neural tube mutant Loop-tail. Nat. Genet. 28, 251–255.

Kohlbecker, A., Lee, A.E., Schorle, H., 2002. Exencephaly in a subset of animals heterozygous for AP-2alpha mutation. Teratology 65, 213–218.

Lawson, A., Anderson, H., Schoenwolf, G.C., 2001. Cellular mechanisms of neural fold formation and morphogenesis in the chick embryo. Anat. Rec. 262, 153–168.

Lohnes, D., Mark, M., Mendelsohn, C., Dolle, P., Dierich, A., Gorry, P., Gansmuller, A., Chambon, P., 1994. Function of the retinoic acid receptors (RARs) during development (I). Craniofacial and skeletal abnormalities in RAR double mutants. Development 120, 2723–2748.

McLeod, M.J., 1980. Differential staining of cartilage and bone in whole mouse fetuses by alcian blue and alizarin red S. Teratology 22, 299–301.

McMahon, J.A., Takada, S., Zimmerman, L.B., Fan, C.M., Harland, R.M., McMahon, A.P., 1998. Noggin-mediated antagonism of BMP signaling is required for growth and patterning of the neural tube and somite. Genes Dev. 12, 1438–1452.

Montcouquiol, M., Rachel, R.A., Lanford, P.J., Copeland, N.G., Jenkins, N.A., Kelley, M.W., 2003. Identification of Vangl2 and Scrb1 as planar polarity genes in mammals. Nature 423, 173–177.

Morriss-Kay, G.M., Tan, S-S., 1987. Mapping cranial neural crest cell migration pathways in mammalian embryos. Trends Genet. 3, 257–261.

Moury, J.D., Schoenwolf, G.C., 1995. Cooperative model of epithelial shaping and bending during avian neurulation: autonomous movements of the neural plate, autonomous movements of the epidermis, and interactions in the neural plate/epidermis transition zone. Dev. Dyn. 204, 323–337.

Murdoch, J.N., Doudney, K., Paternotte, C., Copp, A.J., Stanier, P., 2001. Severe neural tube defects in the loop-tail mouse result from mutation of Lpp 1, a novel gene involved in floor plate specification. Hum. Mol. Genet. 10, 2593–2601.

Murdoch, J.N., Henderson, D.J., Doudney, K., Gaston-Massuet, C., Phillips, H.M., Paternotte, C., Arkell, R., Stanier, P., Copp, A.J., 2003. Disruption of scribble (Scrb1) causes severe neural tube defects in the circletail mouse. Hum. Mol. Genet. 12, 87–98.

Sakai, Y., 1989. Neurulation in the mouse: manner and timing of neural tube closure. Anat. Rec. 223, 194–203.

Santagati, F., Rijli, F.M., 2003. Cranial neural crest and the building of the vertebrate head. Nat. Rev. Neurosci. 4, 806–818.

Sauka-Spengler, T., Bronner-Fraser, M., 2006. Development and evolution of the migratory neural crest: a gene regulatory perspective. Curr. Opin. Genet. Dev. 16, 360–366.

Schorle, H., Meier, P., Buchert, M., Jaenisch, R., Mitchell, P.J., 1996. Transcription factor AP-2 essential for cranial closure and craniofacial development. Nature 381, 235–238.

Schwenk, F., Baron, U., Rajewsky, K., 1995. A cre-transgenic mouse strain for the ubiquitous deletion of loxP-flanked gene segments including deletion in germ cells. Nucleic Acids Res. 23, 5080–5081.

Shum, A.S., Copp, A.J., 1996. Regional differences in morphogenesis of the neuroepithelium suggest multiple mechanisms of spinal neurulation in the mouse. Anat. Embryol. (Berl.) 194, 65–73.

Stottmann, R.W., Berrong, M., Matta, K., Choi, M., Klingensmith, J., 2006. The BMP antagonist Noggin promotes cranial and spinal neurulation by distinct mechanisms. Dev. Biol. 295, 647–663.

Ting, S.B., Wilanowski, T., Auden, A., Hall, M., Voss, A.K., Thomas, T., Parekh, V., Cunningham, J.M., Jane, S.M., 2003a. Inositol- and folate-resistant neural tube defects in mice lacking the epithelial-specific factor Grhl-3. Nat. Med. 9, 1513–1519.

Ting, S.B., Wilanowski, T., Cerruti, L., Zhao, L.L., Cunningham, J.M., Jane, S.M., 2003b. The identification and characterization of human Sister-of-Mammalian Grainyhead (SOM) expands the grainyhead-like family of developmental transcription factors. Biochem. J. 370, 953–962.

Ting, S.B., Caddy, J., Hislop, N., Wilanowski, T., Auden, A., Zhao, L.L., Ellis, S., Kaur, P., Uchida, Y., Holleran, W.M., Elias, P.M., Cunningham, J.M., Jane, S.M., 2005. A homolog of Drosophila grainy head is essential for epidermal integrity in mice. Science 308, 411–413.

Wallingford, J.B., Harland, R.M., 2002. Neural tube closure requires Dishevelled-dependent convergent extension of the midline. Development 129, 5815–5825.

Wang, J., Hamblet, N.S., Mark, S., Dickinson, M.E., Brinkman, B.C., Segil, N., Fraser, S.E., Chen, P., Wallingford, J.B., Wynshaw-Boris, A., 2006. Dishevelled genes mediate a conserved mammalian PCP pathway to regulate convergent extension during neurulation. Development 133, 1767–1778.

Ybot-Gonzalez, P., Cogram, P., Gerrelli, D., Copp, A.J., 2002. Sonic hedgehog and the molecular regulation of mouse neural tube closure. Development 129, 2507–2517.

Ybot-Gonzalez, P., Gaston-Massuet, C., Girdler, G., Klingensmith, J., Arkell, R., Greene, N.D., Copp, A.J., 2007a. Neural plate morphogenesis during mouse neurulation is regulated by antagonism of Bmp signalling. Development 134, 3203–3211.

Ybot-Gonzalez, P., Savery, D., Gerrelli, D., Signore, M., Mitchell, C.E., Faux, C.H., Greene, N.D., Copp, A.J., 2007b. Convergent extension, planar-cell-polarity signalling and initiation of mouse neural tube closure. Development 134, 789–799.

Zhang, H., Bradley, A., 1996. Mice deficient for BMP2 are nonviable and have defects in amnion/chorion and cardiac development. Development 122, 2977–2986.

Zhang, J., Hagopian-Donaldson, S., Serbedzija, G., Elsemore, J., Plehn-Dujowich, D., McMahon, A.P., Flavell, R.A., Williams, T., 1996. Neural tube, skeletal and body wall defects in mice lacking transcription factor AP-2. Nature 381, 238–241.